Progress In Electromagnetics Research C, Vol. 25, 223–232, 2012

THE MEASUREMENT AND ANALYSIS OF WIMAX BASE STATION SIGNAL COVERAGE

Y.-H. Lee [1], H. -W. Tseng [2, *], W.-C. Lee [1], J.-Y. Lin [1], Y.-G. Jan [1], and H.-W. Tsao [3]

[1]Department of Electrical Engineering, Tamkang University, Taipei, Taiwan 251, R.O.C.

[2]Department of Computer and Communication Engineering, De Lin Institute of Technology, Taipei County 236, Taiwan, R.O.C.

[3]Graduate Institute of Communication Engineering, National Taiwan University, Taipei 106, Taiwan, R.O.C.

Abstract—This paper presents the field trial measurement data of WiMAX base station; it includes the system coverage, signal strength and available transmission rate. Data consisting of real time images, VoIP internet telephone are transmitted through Skype software by using WiMAX, HSDPA (3.5G) and EDGE (2G) transmission techniques, and these data are connected to centrally equipped wireless monitoring servers to perform data monitoring and analysis. Finally, we make comparisons, analysis and discussions of these three transmission techniques from the measured and characterized data.

1. INTRODUCTION

With prosperous development of wireless data communication and the maturity of various wire line and wireless communication techniques, the demand for high mobility network, such as HDTV, outdoor networking, HSDPA etc., has been increasing in every dimension; it allows users at any time and anywhere to enjoy high speed networking and receive their request or demand information instantly. However, for users at this high speed information age their demands for wide bandwidth transmission are continuously increasing, and consequently their requests for various services are also flourishing in all fields.

Received 20 July 2011, Accepted 8 October 2011, Scheduled 24 November 2011
* Corresponding author: Hsien-Wei Tseng (hsienwei.tseng@gmail.com).

WiMAX (Worldwide Interoperability for Microwave Access) is a new transmission technology which provides the bandwidth congregation technique in a wider coverage area than WiFi and provides users higher data transmission capacity. WiMAX can provide various applications in mobility and high transmission data rate. With continuous technology improvement and the maturity of system development, it enables to provide more flexibility and better mobility data transmission with WiMAX platform.

HSDPA (High Speed Downlink Packet Access) is a mobile communication protocol. It is also called 3.5G, and the throughput is up to $8 \sim 10$ Mbit/s. Enhanced data rates for GSM evolution (EDGE) is an extension of 2G and 2.5G (GPRS). The maximum throughput is 384 Kbps.

The remaining paper is organized in the following. Section 2 introduces the WiMAX signal measurement environments. Section 3 compares the measurement data and simulation results in WiMAX, and the signal qualities of WiMAX/HSDPA/EDGE are compared. The conclusion is drawn in Section 4.

Table 1. IEEE 802.16m system parameters [2].

Parameters	Values				
System bandwidth (MHz)	1.25	2.5	5	10	20
Sampling frequency (Fs, MHz)	1.429	2.857	5.714	11.429	22.857
Sample time (1/Fs, nsec)	700	350	175	88	44
FFT size (NFFT)	128	256	512	1024	2048
Subcarrier frequency pacing	11.16 KHz				
Useful symbol time (Tb=1/f)	89.6 μs				
Guard time (Tg=Tb/8)	11.2 μs				
OFDM symbol time (Ts=Tb+Tg)	100.8 μs				

2. MEASUREMENT OF WIMAX SIGNAL

The WiMAX operating frequency band in Taiwan is deployed in $2.50 \sim 2.69\,\mathrm{GHz}$ [1–3]. The system parameters of IEEE 802.16m standard with possible system bandwidths are listed in Table 1, while Table 2 tabulates the relationship between the frame duration and frame size for every system bandwidth considered in Table 1.

The WiMAX base station is set up on the thirteenth floor of the International Building at the National Taiwan University of Science and Technology, and its coverage range includes the campus of the National Taiwan University as shown in Figure 1.

Totally fifty-eight (58) locations have been selected as the test points for WiMAX measurements, including certain main streets and buildings in the main campus of the National Taiwan University. After integrating the measurement results from these fifty-eight test locations, the WiMAX received signal strengths in its coverage range have a distribution as shown in Figure 2. In Figure 2, different colors are used to identify various RSSI levels and their associated throughput in the system coverage range. Areas identified with light gray color are the areas having the best signal quality with RSSI larger than $-60\,\mathrm{dBm}$, while areas with gray color indicate that the signal strengths in these areas are between $-60 \sim -80\,\mathrm{dBm}$, and the areas with the worst signal quality with RSSI less than $-80\,\mathrm{dBm}$ are indicated by griseous color, and the signal may be imminently cut off. The resulting system downlink throughput, CINR (carrier to interference and noise ratio), and RSSI in each coverage area is summarized in Table 3 for comparison.

Table 2. Relation between frame duration and frame size.

Frame size (ms)	Frame size (symbols/s)
2	19
2.5	24
4	39
5	49
8	79
10	99
12.5	124
20	198

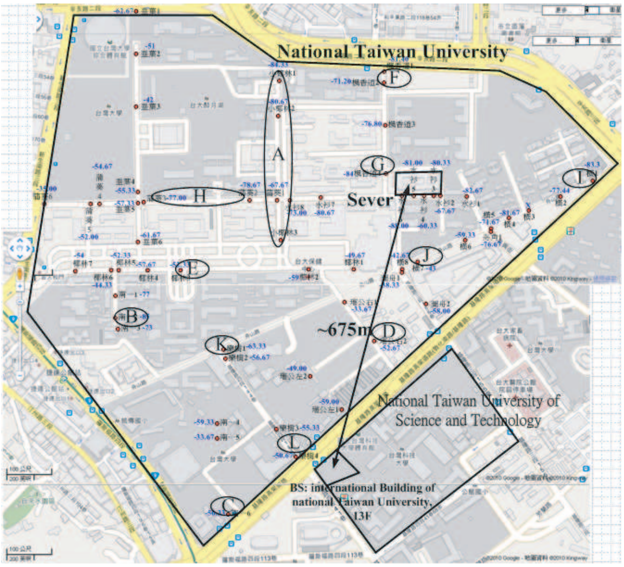

Figure 1. WiMAX base station (VMAX).

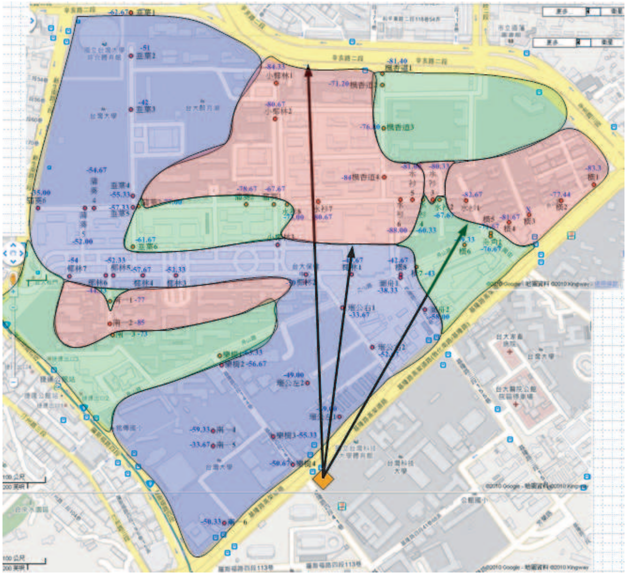

Figure 2. WiMAX base station signal strength distributions.

Table 3. WiMAX coverage.

Color	Modulation	DL Throughput (Mbps)	CINR (dB)	RSSI (dBm)
Red	QPSK	2.03	9.18	−82.71
Green	16 QAM	3.27	11.32	−73.95
Blue	64 QAM	3.91	23.65	−51.26

3. ANALYSIS OF MEASURED DATA AND SIMULATION TEST

3.1. Channel Model [4–13]

In wireless transmission, the received signal strength will be affected by many factors such as channel noise, antenna configuration and its gain, multipath effect due to the signal being obstructed when it passes through the buildings, woods and terrain reflection, etc. Especially, the multipath fading effect will make the received signal vary randomly. The communication channel is then analyzed and simulated through the channel statistical characteristics, and many channel models have been proposed and discussed. The signal strength at the receiver terminal can be summarized in the following equation:

$$P(\text{dBm}) = P_t + G_t + G_r - PL \tag{1}$$

where

P_t: Transmitting power of base station/ mobile station (dBm).

G_t: Antenna gain of mobile station /base station (dBi).

G_r: Antenna gain of base station/ mobile station (dBi).

PL is the path loss in dB between the transmitter and the receiver

The path loss model considered in this paper follows the Macro-cell COST 231 Hata model as shown in the following equation when the user is equipped with an antenna with a height of 1.5 meter [14]:

$$\begin{aligned} PL =&(4.49 - 6.55 \log 10(h_{BS})) \log 10(d) + 26.46 + 5.83 \log 10(h_{BS}) \\ &+ 26 \log 10(f[\text{GHz}]/2) \end{aligned} \tag{2}$$

where

d: Transmission distance between the transmitter and the receiver in meters, $10\,\text{m} < d < 5000\,\text{m}$.

h_{BS}: Base station antenna height, $10\,\text{m} < h_{BS} < 150\,\text{m}$.

f: Carrier frequency (GHz), $2\,\text{GHz} \sim 6\,\text{GHz}$.

From Equations (1) and (2), the received signal strength can be determined when the transmission distance between the transmitter and receiver, and other system parameters are given. The resulting system performance can then be estimated when the signal to noise ratio, *SNR*, at the receiver terminal can be measured or calculated.

The noise power can be determined from the following equation:

$$N(\mathrm{dBm}) = N_0 \times BW = kT_e \times BW = BW\frac{4.0\,\mathrm{pW}}{\mathrm{GHz}} \tag{3}$$

where

$$\begin{aligned} k &= 1.38 \times 10^{-23} J/K \;\; (\text{Boltzmann constant}) \\ T_e &= 273 + {}^\circ\mathrm{C} \end{aligned}$$

BW is the system bandwidth.

The resulting *SNR* can be calculated from the following equation,

$$SNR(\mathrm{dB}) = P(\mathrm{dBm}) - N(\mathrm{dBm}) \tag{4}$$

3.2. Measured Data and Simulation Test

With the system parameters as listed in Table 4 used in the system simulation, the resulting simulated system downlink throughput in WiMAX is as shown in Figure 3. It shows that the system can provide up to 10 Mbps in downlink throughput with 16 QAM or 64 QAM modulation while it can generate only 4 Mbps throughput for the QPSK modulation mapping. The field trial measurement has data as shown in Figure 4. Comparing actual measurements from simulations in all test cases, with results plotted in Figures 3 and 4, the actual measurements appear to have lower throughput than the simulation

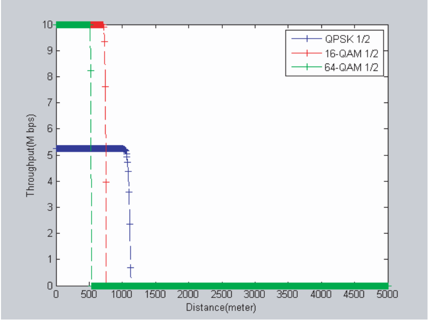

Figure 3. Simulated downlink throughput of WiMAX.

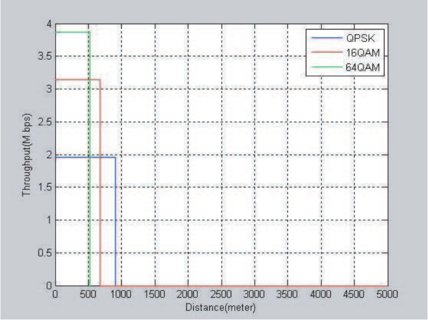

Figure 4. Measured downlink throughput of WiMAX.

Table 4. System simulation parameters of WiMAX.

Channel Bandwidth (MHz)	10
FFT Size	1024
Sampling frequency, Fs (MHz)	11.2
Subcarrier spacing (kHz)	10.94
Useful symbol time, Tb (μs)	91.4
Number of Subcarrier	768
Coding Rate	1/2
Modulation	QPSK, 16 QAM, 64 QAM
Transmitter Power	1 Watt (30 dBm)

Table 5. Comparison of measured and simulated downlink throughput of WiMAX.

	Simulation		Measured	
	Throughput-*BS*	Distance	Throughput-CPE	Distance
QPSK	5.2 Mbps	1130 m	1.96 Mbps	909.8 m
16 QAM	10 Mbps	755 m	3.14 Mbps	672.1 m
64 QAM	10 Mbps	560 m	3.86 Mbps	524.6 m

results, which may be due to the non-ideal channel model encountered in the field trail measurement. The difference between the measured and simulated results, i.e., the difference between Figures 3 and 4, is tabulated in Table 5.

3.3. Simulation Results Of WiMAX, HSDPA Or EDGE

Figure 5 shows the system simulation functional block diagram for WiMAX, HSPDA or EDGE. The Server is set up on the fifth floor of the Electrical Engineering Building II at the National Taiwan University. The WiMAX base station is located on the thirteenth floor of the International Building at the National Taiwan University of Science and Technology. It is 675 meters away from the server and connects to the wireless network of WiMAX, 3.5G HSDPA/WCDMA or 2G EDGE through the selection of WiMAX Dongle and 3.5G/2G Dongle.

The measurements at test points, $A \sim L$, as shown in Figure 1 have been performed. The test points B, G and I are operated for the indoor test while test points A, C, D, E, F, H, J, K and L are

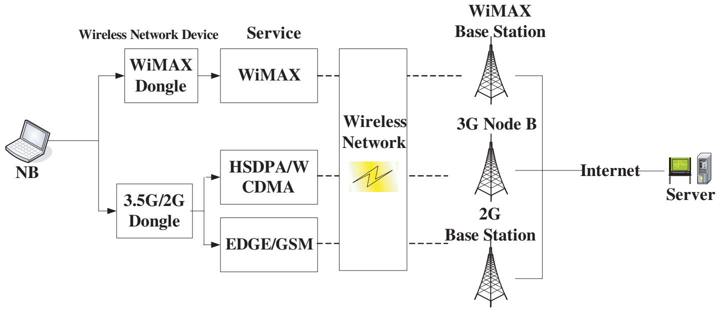

Figure 5. Functional block diagram for system performance simulation.

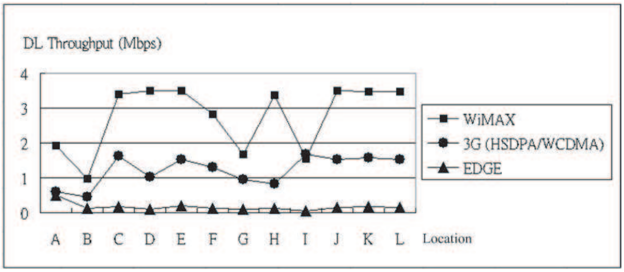

Figure 6. Downlink Throughput comparisons.

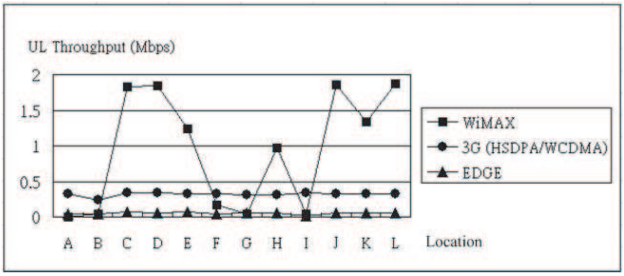

Figure 7. Uplink throughput comparisons

operated for the outdoor test. From the simulation results as shown in Figures 6 and 7, the WiMAX has the throughput almost double as that of the 3.5G system, almost ten times as that of EDGE. At the receiving locations with stronger signal strengths, the WiMAX has the highest DL throughput. However, in the UL measurements it has different throughput from that of DL measurement. When the WiMAX signal strength becomes low, the UL throughput may be dropped to tenth of its highest throughput, and when the signal strength is lower further, the users may be unable to transmit their data reaching to the server.

4. CONCLUSION

The WiMAX system in Taiwan operates in the $2.50 \sim 2.69$ GHz band. The signal strength in indoor transmission fades significantly as validated from the field trials measurements data. WiMAX indoor transmission needs to manipulate with other apparatuses such as repeater, pico, femto cell etc. to improve the signal quality or extend the system coverage range. From our measurement results, we could make the following recommendation: if WiMAX system is deployed outdoor but not having satisfactory indoor signal coverage and meanwhile only a few users are indoor, then we recommend the exploitation of repeaters to improve the indoor signal quality. If it is an indoor small office or residence but it has more than five users then it recommends installing femto cells. If it is an office building and it has more than ten users then it is appropriate to use pico cell to improve the signal quality. How the signal quality is improved when any of these recommendations is implemented in the WiMAX system is our ongoing project. When more data are available in various WiMAX system structures, the transmission characteristics of each WiMAX system will be revealed and discussed properly.

ACKNOWLEDGMENT

The authors would like to express their sincere thanks to Sheng-Han Hung and Jheng-Wei Lee. This study is partially supported by the National Science Council, ROC under contracts NSC 100-2219-E-002-019, NSC 100-2221-E-032 -031, and NSC 100-2219-E-009 -027.

REFERENCES

1. Eklund, C., R. B. Marks, K. Stanwood, and S. Wang, "IEEE standard 802.16: A technical overview of the wireless MANTM air interface for broadband wireless access," *IEEE Commun. Magazine*, Vol. 6, No. 6, 98–107, Jun. 2002.
2. IEEE 802.16 Broadband Wireless Access Working Group, "IEEE Standard for local and metropolitan area networks, part 16: Air interface for broadband wireless access systems, amendment 3: Advanced air interface," IEEE Std 802.16 m$^{\mathrm{TM}}$, 2011.

3. Yaghoobi, H., "Scalable OFDMA physical layer in IEEE 802.16 wireless MAN," *Intel Technology Journal*, Vol. 8, No. 3, Intel Communications Group, Intel Corporation, 2004.
4. IEEE 802.16 Broadband Wireless Access Working Group, *IEEE 802.16m evaluation methodology document (EMD)*, IEEE 802.16 Working Group on Broadband Wireless Access Standards, IEEE 802.16m-08/004r5, Jan. 2009.
5. Hoymann, C., "Analysis and performance evaluation of the OFDM-based metropolitan area network IEEE 802.16," *The International Journal of Computer and Telecommunications Networking*, Vol. 49, 341–363, Oct. 2005.
6. Erceg, V., K. V. S. Hari, M. S. Smith, D. S. Baum, and P. Soma, "Channel models for fixed wireless applications," IEEE 802.16 Broadband Wireless Access Working Group, C802.16.3c-01/29r4, Jun. 2003.
7. Andreas, F. M. , H. Asplund, R. Heddergott, M. Steinbauer, and T. Zwick, "The COST259 directional channel model - I: Overview and methodology," *IEEE Trans. on Wireless Communications*, Vol. 5, 3421–3433, 2006.
8. Steinbauer, M., A. F. Molisch, and E. Bonek, "The double-directional radio channel," *IEEE Antennas and Propagation Magazine*, 51–63, Aug. 2001.
9. Foschini, G. J. and M. J. Gans, "On limits of wireless communications in a fading environment when using multiple antennas," *Wireless Personal Communications*, Vol. 6, 311–335, Feb. 1998.
10. Lee, Y.-H., Y.-G. Jan, L. Wang, Q. Chen, Q. W. Yuan, and K. Sawaya, "Using hopping technique for interference mitigation in modulated scattering array antenna system" *IEICE Electronics Express*, Vol. 7, No. 12, 839–843, 2010 (SCI, EI, Engineering).
11. Lee, Y.-H., Y.-G.Jan, H. Huang, Q. Chen, Q. W. Yuan, and K. Sawaya, "Using LDPC coding and AMC to mitigate received power imbalance in carrier aggregation communication system," *IEICE Electronics Express*, Vol. 8, No. 8, 618–622, 2011.
12. Stallings, W., *Wireless Communications and Networks*, Prentice-Hall, 2002.
13. COST Action 231, *Digital Mobile Radio Towards Future Generation Systems, Final Report*, Tech., Rep., European Communities, EUR 18957, 1999.
14. Rel.9 3GPP TR 36.814 "Further advancements for E-UTRA physical layer aspects," Mar. 2010.